

## Dielectron production: QGP versus photon-photon mechanism

---

Wolfgang Schäfer<sup>a,\*</sup>

<sup>a</sup>*Institute of Nuclear Physics Polish Academy of Sciences  
ul. Radzikowskiego 152, Kraków, Poland*

*E-mail:* [wolfgang.schafer@ifj.edu.pl](mailto:wolfgang.schafer@ifj.edu.pl)

We summarize recent work, where we calculated the cross sections for dilepton production by photon-photon processes in ultrarelativistic heavy-ion collisions from low (SPS) to high (LHC) energy. We concentrate on very low pair transverse momenta,  $P_T < 0.15$  GeV. Specifically, we investigate the interplay of thermal radiation with initial photon annihilation processes,  $\gamma\gamma \rightarrow l^+l^-$ , triggered by the coherent electromagnetic fields of the incoming nuclei. For the thermal radiation, we employ the emission from the QGP and hadronic phases with in-medium vector spectral functions which describes the inclusive excess radiation observed over a wide range of collision energies.

We also discuss an approach to the impact-parameter dependent  $P_T$ -distribution of lepton pairs, which involves a Wigner transform of the density matrix of Weizsäcker–Williams photons.

*40th International Conference on High Energy physics - ICHEP2020  
July 28 - August 6, 2020  
Prague, Czech Republic (virtual meeting)*

---

\*Speaker

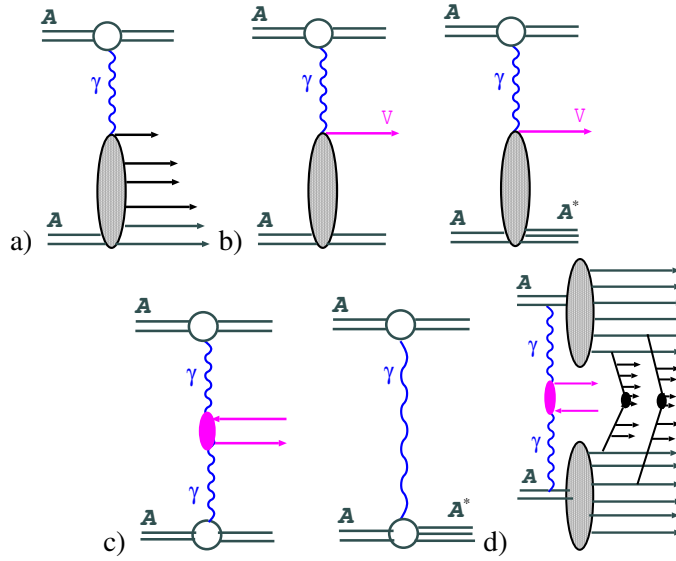


**Figure 1:** a)-c): typical Feynman diagrams relevant for ultraperipheral Heavy-Ion collisions. d): coherent photon cloud contribution in inelastic nuclear collisions.

## 1. Weizsäcker Williams fluxes - from ultraperipheral to semicentral collisions

The large, enhanced by the square of the ion's charge  $Z^2$ , flux of Weizsäcker–Williams photons accompanying ultrarelativistic heavy ions opens up the opportunity to study a variety of photon-induced nuclear processes, as well as photon-photon processes. See for example the reviews with focus on RHIC and LHC [1]. Some possible processes are depicted in Fig. 1. They include generic inelastic photon-nucleus processes with production of many hadrons (Fig. 1 a), diffractive coherent and incoherent production of vector mesons (Fig. 1 b). There also is a range of processes without production of particles via the strong interactions, such as dilepton production by  $\gamma\gamma$ -fusion or electromagnetic excitation and dissociation of nuclei e.g. by the excitation of Giant Dipole Resonances. These processes are generally associated with ultraperipheral collisions, where each of the exchanged photons in the diagrams shown in Fig. 1(a-c) is associated with a large rapidity gap. The coherent cloud of Weizsäcker-Williams photons is characterized by very small transverse momenta  $|q|R_A \ll 1$  of exchanged photons. This translates into very small  $p_T$  of the photoproduced state.

We can regard the Weizsäcker–Williams photons as partons of the nucleus, and it is natural to ask if they play a role also in inelastic collisions. Given that strong interactions are short range, these processes occur if the colliding nuclei overlap geometrically in the impact parameter plane. In this case, the strongly interacting nuclei give rise to an “underlying event, in which e.g. plasma can be formed (Fig. 1 d). The relevance of coherent photons in this case has been discussed already some time ago [2]. Recently, the STAR collaboration at RHIC has measured dilepton pairs in three centrality classes down to very small  $P_T$  of the pair and observes a large enhancement for  $P_T < 150$  MeV.

Dileptons are a “classic” probe of the strongly interacting matter/ quark gluon plasma (QGP) produced in the collision, see for example Ref. [4] for reviews. A part of the spectrum carries

information on the medium modifications of light vector mesons, and there is also a contribution of thermal dileptons. In Ref. [5], we investigated the interplay between the different mechanisms. Here the calculation of thermal dilepton production from a near-equilibrated medium follows the approach of [6]. The calculation of the coherent photon contribution is set up in impact parameter space. The relevant cross section is obtained from a convolution of the standard Weizsäcker-Williams fluxes, which as an input need only the nuclear charge form factor:

$$\frac{d\sigma_{ll}}{d\xi d^2\mathbf{b}} = \int d^2\mathbf{b}_1 d^2\mathbf{b}_2 \delta^{(2)}(\mathbf{b} - \mathbf{b}_1 - \mathbf{b}_2) N(\omega_1, b_1) N(\omega_2, b_2) \frac{d\sigma(\gamma\gamma \rightarrow l^+l^-; \hat{s})}{d(-\hat{t})}. \quad (1)$$

Here the phase space element is  $d\xi = dy_+ dy_- dp_t^2$  with  $y_{\pm}$ ,  $p_t$  and  $m_l$  the single-lepton rapidities, transverse momentum and mass, respectively. The photon energies  $\omega_{1,2}$  are fixed by the lepton momenta. The yield in a given centrality class  $C$  is given by

$$\frac{dN_{ll}[C]}{dM} = \frac{1}{f_C \cdot \sigma_{AA}^{\text{in}}} \int_{b_{\text{min}}}^{b_{\text{max}}} db \int d\xi \delta(M - 2\sqrt{\omega_1\omega_2}) \left. \frac{d\sigma_{ll}}{d\xi db} \right|_{\text{cuts}}, \quad (2)$$

where the relevant impact parameter ranges can be obtained by a simple optical limit Glauber calculation, and  $f_C$  is the fraction of inelastic events in the centrality bin  $C$ . In Fig. 2 we show our results for the invariant mass distribution of dileptons in three different centrality classes and compare them to the data by the STAR collaboration. We observe that in the most peripheral bin, the photon-induced dileptons almost exhaust the cross section. They dominate also in the 40-60% centrality range, whereas for the most central bin, thermal dileptons and hadronic cocktail contribute in similar amounts. In the left panel of Fig. 3 we show the situation for the energy range of the SPS. Evidently, here the in-medium  $\rho$  meson and QGP contributions dominate. It is interesting to look at the evolution of the interplay of the different mechanisms with energy. In the right panel of Fig. 3 we see that thermal emission rises logarithmically with energy, while the  $\gamma\gamma$  process is strongly energy dependent for  $\sqrt{s_{NN}} < 100$  GeV and levels off roughly above RHIC energy.

In the left panel of Fig.4 we show the distribution in dilepton transverse momentum. The photoproduction contribution stands out clearly as a peak for  $P_T < 0.15$  GeV. Our calculation was performed as a convolution of the transverse momentum-dependent photon fluxes,

$$\frac{dN(\omega, \mathbf{q})}{d^2\mathbf{q}} \propto |E(\omega, \mathbf{q})|^2, \quad \text{with } E(\omega, \mathbf{q}) \propto \frac{\mathbf{q} F_{\text{ch}}(\mathbf{q}^2 + \omega^2/\gamma^2)}{\mathbf{q}^2 + \frac{\omega^2}{\gamma^2}}. \quad (3)$$

The photoproduction predictions agree reasonably well with data, although they peak at slightly lower  $P_T$  than data. In fact, with increasing cm-energy, the peak would run away towards smaller and smaller  $P_T$ , because  $\omega/\gamma$  in Eq. 3 decreases with increasing boost parameter  $\gamma$ .

## 2. Wigner transform of the photon polarization density matrix

Up to now we neglected the correlation between photon transverse momenta and the impact parameter of the collision. For a simultaneous description in momentum and configuration space a formulation based on Wigner-functions is appropriate. We briefly discuss preliminary results of

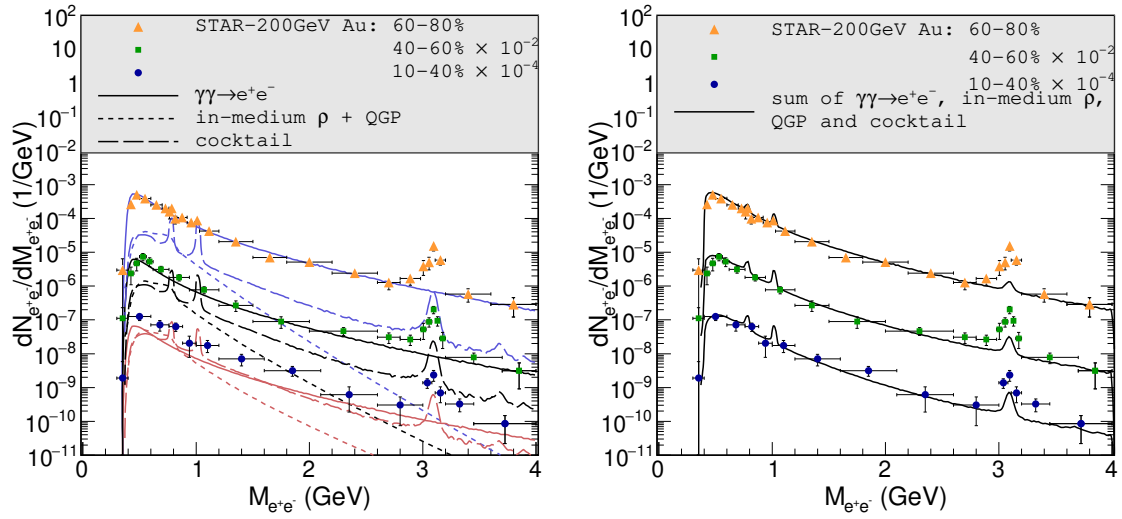


**Figure 2:** Left panel: Dielectron invariant-mass spectra for pair- $P_T < 0.15$  GeV in Au+Au ( $\sqrt{s_{NN}}=200$  GeV) collisions for 3 centrality classes including experimental acceptance cuts ( $p_t > 0.2$  GeV,  $|\eta_e| < 1$  and  $|y_{e^+e^-}| < 1$ ) for  $\gamma\gamma$  fusion (solid lines), thermal radiation (dotted lines) and the hadronic cocktail (dashed lines); right panel: comparison of the total sum (solid lines) to STAR data [3].

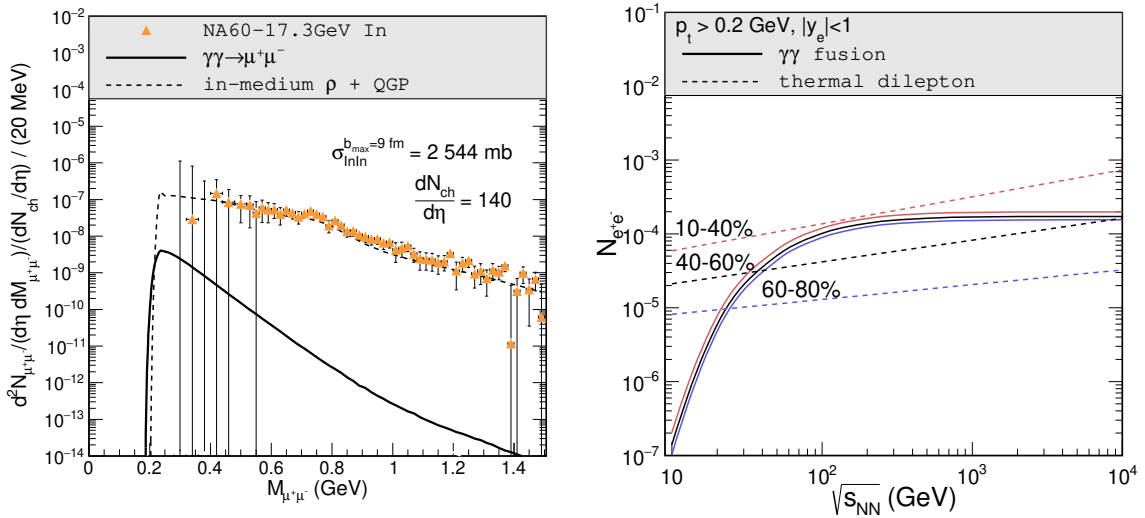


**Figure 3:** Left panel: Low- $P_T$  ( $< 0.2$  GeV) acceptance-corrected dimuon invariant mass excess spectra in the rapidity range  $3.3 < Y_{\mu^+\mu^-}, LAB < 4.2$  for In+In ( $\sqrt{s_{NN}}=17.3$  GeV) collisions at the SPS. Calculations for coherent  $\gamma\gamma$  fusion (solid line) and thermal radiation (dashed line) are compared to NA60 data [7]. Right panel: Excitation function of low- $P_T$  ( $< 0.15$  GeV) dilepton yields from  $\gamma\gamma$  fusion (solid lines) and thermal radiation (dashed lines) in collisions of heavy nuclei ( $A \approx 200$ ) around midrapidity in three centrality classes, including single- $e^\pm$  acceptance cuts.

our ongoing work [8].<sup>1</sup> More precisely, the relevant ingredient for the factorization formula is a

<sup>1</sup>An approach to dilepton production based on Wigner functions has recently been proposed in [9]

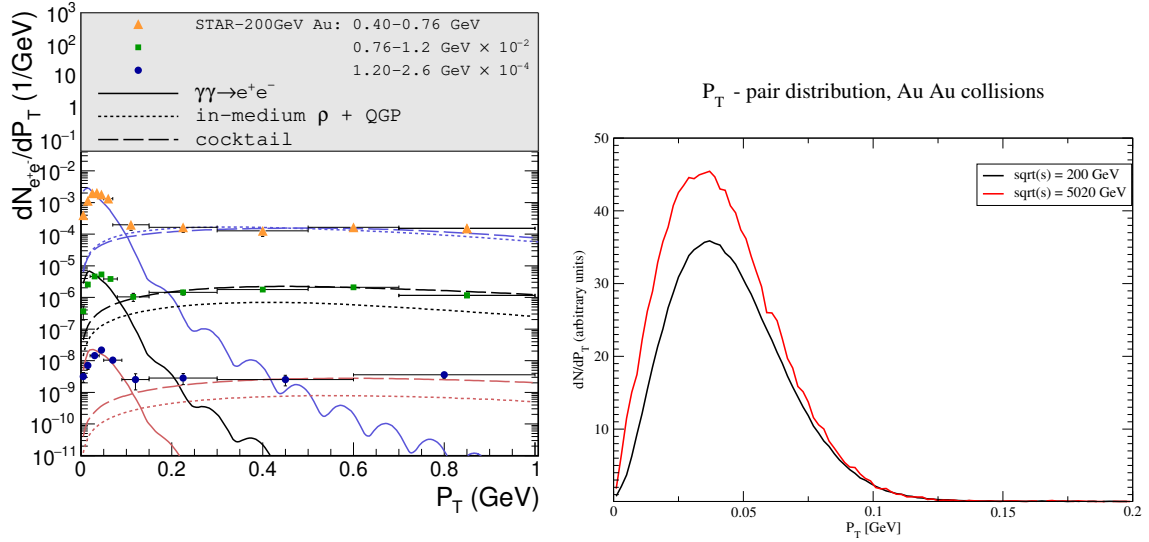


**Figure 4:** Left panel:  $P_T$  spectra of the individual contributions (line styles as in the previous figure) in 3 different mass bins for 60-80% central Au+Au collisions ( $\sqrt{s_{NN}}=200$  GeV), compared to STAR data [3]. Right panel:  $P_T$  spectra for 60-80% central Au+Au collisions ( $\sqrt{s_{NN}}=200$  GeV, 5020 GeV).

Wigner transform of a polarization density matrix of Weizsäcker–Williams photons:

$$N_{ij}(\omega, \mathbf{b}, \mathbf{q}) = \int \frac{d^2\mathbf{Q}}{(2\pi)^2} \exp[-i\mathbf{b}\mathbf{Q}] E_i\left(\omega, \mathbf{q} + \frac{\mathbf{Q}}{2}\right) E_j^*\left(\omega, \mathbf{q} - \frac{\mathbf{Q}}{2}\right). \quad (4)$$

Here  $i, j$  are cartesian polarizations of photons. The cross section can be cast into a form which involves cross sections for photons in channels of angular momentum projection  $J_z = 0, \pm 2$  and even or odd parity:

$$\begin{aligned} \frac{d\sigma}{d^2\mathbf{b}d^2\mathbf{P}} &= \int \frac{d^2\mathbf{Q}}{(2\pi)^2} \exp[-i\mathbf{b}\mathbf{Q}] \int \frac{d\omega_1}{\omega_1} \frac{d\omega_2}{\omega_2} \int \frac{d^2\mathbf{q}_1}{\pi} \frac{d^2\mathbf{q}_2}{\pi} \delta^{(2)}(\mathbf{P} - \mathbf{q}_1 - \mathbf{q}_2) \\ &\times E_i\left(\omega_1, \mathbf{q}_1 + \frac{\mathbf{Q}}{2}\right) E_j^*\left(\omega_1, \mathbf{q}_1 - \frac{\mathbf{Q}}{2}\right) E_k\left(\omega_2, \mathbf{q}_2 - \frac{\mathbf{Q}}{2}\right) E_l^*\left(\omega_2, \mathbf{q}_2 + \frac{\mathbf{Q}}{2}\right) \\ &\times \frac{1}{2\hat{s}} \left\{ \delta_{ik}\delta_{jl} \sum_{\lambda\bar{\lambda}} \left| M_{\lambda\bar{\lambda}}^{(0,+)} \right|^2 + \epsilon_{ik}\epsilon_{jl} \sum_{\lambda\bar{\lambda}} \left| M_{\lambda\bar{\lambda}}^{(0,-)} \right|^2 \right. \\ &\left. + P_{ik}^{\parallel} P_{jl}^{\parallel} \sum_{\lambda\bar{\lambda}} \left| M_{\lambda\bar{\lambda}}^{(2,-)} \right|^2 + P_{ik}^{\perp} P_{jl}^{\perp} \sum_{\lambda\bar{\lambda}} \left| M_{\lambda\bar{\lambda}}^{(2,+)} \right|^2 \right\} d\Phi(l^+l^-). \end{aligned} \quad (5)$$

with  $\delta_{ik} = \hat{x}_i\hat{x}_k + \hat{y}_i\hat{y}_k$ ,  $\epsilon_{ik} = \hat{x}_i\hat{y}_k - \hat{y}_i\hat{x}_k$ ,  $P_{ik}^{\parallel} = \hat{x}_i\hat{x}_k - \hat{y}_i\hat{y}_k$ ,  $P_{ik}^{\perp} = \hat{x}_i\hat{y}_k + \hat{y}_i\hat{x}_k$ . In the right panel of Fig. 4 we show the  $P_T$  distribution of dileptons for RHIC and LHC energies. We see that the position of the peak no longer runs away to low  $P_T$ .

### 3. Summary

We have studied low- $P_T$  dilepton production in ultrarelativistic heavy-ion collisions, by a systematic comparisons of thermal radiation, the “hadronic cocktail” and photon-photon fusion

within the coherent fields of the incoming nuclei. Comparison to recent STAR data shows a good description of low- $P_T$  dilepton data in Au+Au ( $\sqrt{s_{NN}}=200$  GeV) collisions in three centrality classes, for invariant masses from threshold to  $\sim 4$  GeV. Coherent emission dominates for the two peripheral samples, and is comparable to the cocktail and thermal radiation yields in semi-central collisions. At SPS energies ( $\sqrt{s_{NN}}=17.3$  GeV) we found that the  $\gamma\gamma$  contribution is subleading. The impact-parameter dependent dilepton  $P_T$  distribution is described by a density matrix generalization of the Weizsäcker-Williams fluxes. Channels of  $J_z = 0, \pm 2$  enter with different weights. For  $e^+e^-$  pairs the  $J_z = \pm 2$  channels dominate.

## Acknowledgements

This work was partially supported by the Polish National Science Center under grant No. 2018/31/B/ST2/03537

## References

- [1] G. Baur, K. Hencken, D. Trautmann, S. Sadovsky and Y. Kharlov, Phys. Rept. **364** (2002), 359-450 [arXiv:hep-ph/0112211 [hep-ph]]; S. Klein and P. Steinberg, Ann. Rev. Nucl. Part. Sci. **70**, 323-354 (2020) [arXiv:2005.01872 [nucl-ex]]; W. Schäfer, Eur. Phys. J. A **56** (2020) no.9, 231.
- [2] N. Baron and G. Baur, Z. Phys. C **60** (1993), 95-100.
- [3] J. Adam *et al.* [STAR], Phys. Rev. Lett. **121** (2018) no.13, 132301 [arXiv:1806.02295 [hep-ex]].
- [4] I. Tserruya, Landolt-Bornstein **23** (2010), 176 [arXiv:0903.0415 [nucl-ex]]; R. Rapp, Adv. High Energy Phys. **2013** (2013), 148253 [arXiv:1304.2309 [hep-ph]].
- [5] M. Klusek-Gawenda, R. Rapp, W. Schäfer and A. Szczurek, Phys. Lett. B **790** (2019), 339-344 [arXiv:1809.07049 [nucl-th]].
- [6] R. Rapp and E. V. Shuryak, Phys. Lett. B **473** (2000), 13-19 [arXiv:hep-ph/9909348 [hep-ph]].
- [7] R. Arnaldi *et al.* [NA60], Eur. Phys. J. C **61** (2009), 711-720 [arXiv:0812.3053 [nucl-ex]].
- [8] M. Klusek-Gawenda, W. Schäfer and A. Szczurek, a paper in preparation.
- [9] S. Klein, A. H. Mueller, B. W. Xiao and F. Yuan, Phys. Rev. D **102** (2020) no.9, 094013 [arXiv:2003.02947 [hep-ph]].